Bull. Spec. Astrophys. Obs., 2001, 52, 134-144

DATA ON 2-D SPECTROSCOPY

Dynamical modeling of SB galaxies

A.V. Khoperskov[a], A.V. Moiseev[b], E.A. Chulanova[a]

[a] Volgograd State University, Volgograd 400062, Russia
[b] Special Astrophysical Observatory of the Russian AS, Nizhnij Arkhyz 369167, Russia

Abstract. Using the method of N-bodies dynamical modeling distributions of different components of the galaxy stellar disk velocity dispersion have been derived. The velocity dispersion observed along the line of sight is strongly dependent on the galaxy inclination angle and on the mutual orientation of the bar and the disk major axis. The non-symmetric structures in the velocity dispersion distribution are shown to be 2–3 times as small as the sizes of the bar determined from the surface density. Dynamical models of individual SB galaxies (NGC 936, 1169, 2712) are constructed. The observed kinematic (rotation curves of the gaseous and stellar components, radial distribution of the velocity dispersion of stars) and photometric data admit an assumption that the classical gravitation instability of the global bar-mode in the stellar disk is responsible for the origin of bar structures in these objects, and the bar lifetime may be very long. The dynamical modeling makes it possible to investigate into non-stationary structures the lifetime of which is relatively short and which are observed only in the part of galaxies passing a particular evolution phase. Perhaps double-barred stellar disks belong to such objects.

Key words: galaxies: structure — galaxies: individual: SB galaxies — methods: numerical

1. Introduction

Observations made over the last few years have increased the relative proportion of stellar systems with bar-like structures. A descriptive example is the Milky Way, the central bar of which was discovered in the early 1990s (Weinberg, 1992). No understanding of the galactic morphology is possible without realizing that the galaxies are basically dynamical systems. The origin of spiral arms, bars, rings and other galactic structures can be understood only in terms of collective processes of gravitating medium. To reveal physical mechanisms, one has to know the spatial 2D/3D distribution not only of the luminosity but also of the kinematic parameters — velocity fields of stars and gas, velocity dispersion of stars and gas. By the present time the observational techniques have reached the level when spectral investigations can provide detailed kinematic information about the stellar population. Such an opportunity is provided by 2D spectroscopy of galaxies which is usefully complemented by numerical dynamical 3D modeling. By the dynamical modeling we will mean the numerical solution of equations of motion of gravitating N-bodies with allowance made for the external potential.

The non-axisymmetric distribution of matter and potential has an effect on the periphery of galaxies. There exists the point of view that a bar generates a spiral pattern in a disk. However, numerous observed SB0 galaxies without any noticeable spiral pattern give rise to a question: why is the matter outside the bar distributed axially-symmetric? This is undoubtedly associated with the absence of the gaseous component. Even a powerful bar without a gas-dynamical subsystem is unable to create a long-lived stellar spiral pattern of large amplitude. This is illustrated by dynamical modeling. As an example, we have constructed a dynamical model of the SB0 galaxy NGC 936.

Several mechanisms of the origin of a bar has been suggested. The main mechanisms are the gravitation instability of the global bar-mode (Ostriker & Peebles, 1973) and the instability of radial orbits (Polyachenko, 1992). The parameters of a bar are affected by various factors: interaction with the gaseous subsystem and interactions bar/bulge and bar/halo. One of the key points in establishing the mechanism of formation of the central bar is determination of the corotation radius r_c from the equality $\Omega(r_c) = \Omega_{bar}$. The algorithm of Tremaine & Weinberg (1984) of cal-

culation of the angular velocity of the bar, Ω_{bar}, in the processing of the results of dynamical modeling is lacking errors that arise when using the observational data. If a galaxy contains regions of pronounced star formation, then the continuity equation that forms the basis of the method is disturbed because the gas transits into the stars. A second source of errors is the variation in brightness distribution caused by the presence of dust (Merrifield & Kuijken, 1995). As the interaction of the bar and the spheroidal subsystem is disregarded, in the case of establishing quasistationary rotation $r_{bar} \lesssim r_c$ (r_{bar} is the semimajor axis of the bar). Dynamical friction of the bar against the halo leads to angular moment transfer and decelerates rotation of the disk component.

The existence of galaxies without a bar is an argument either for a massive spheroidal subsystem or strong overheating of the stellar disk, which manifests itself in large values of the velocity dispersions of stars. An estimate of maximum dispersions of radial velocities at which stabilization of the global bar-mode occurs is obtained in Section 3 within the frames of dynamical models. This critical value depends on the ratio of the disk mass M_d to halo mass M_h within a fixed radius. It is shown that the existence of a long-lived global bar-mode in stellar disks of galaxies without a bar is possible at large values of the mass of halo, $M_h/M_d \lesssim 3$, depending on the law of density distribution in a spheroidal subsystem. It should be emphasized that bulges can be efficient stabilizers of a bar-mode (Kalnajs, 1987).

From the results of dynamical modeling, spatial distributions of dispersions of different components of velocities of stars with the presence of a bar-mode have been derived. Three dispersion components, c_r, c_φ, c_z, have different distributions. This should be taken into account when analysing the velocity dispersion of stars along the line of sight.

The discovery of double bars in the centres of galaxies poses a problem of studying physical mechanisms of formation of such structures. Numerical simulation shows that double bars can be formed in a stellar disk. These structures, however, prove to be non-stationary and short-lived. Their characteristic lifetime is generally no longer than the period of rotation. As a result, only one bar remains. It is possible that the observed double bars refer to the initial stage of formation of an SB galaxy or to its short phase. This can explain the low frequency of occurrence of double bars.

2. Dynamical models

Consider the dynamics of gravitating N-bodies, which is defined by the set of equations

$$\frac{d^2\vec{r}_i}{dt^2} = \sum_j \vec{f}_{ij} + \vec{F}_s \quad (i = 1, ..., N),$$

the force $\vec{f}_{ij}$ determines interaction between ith and jth particles, the force $\vec{F}_s = \vec{F}_h + \vec{F}_b$ results from the spheroidal subsystem bulge/halo. We will assume that in numerical models $G = 1$. The distribution of matter in the halo $\varrho_h(r) = \varrho_{h0}/(1 + (r/a)^2)$ at $\varrho_{h0} = M_h/\{4\pi a^3[R/a - \mathrm{arctg}(R/a)]\}$ yields the force

$$\vec{F}_h = -\frac{4\pi a^3 \varrho_{h0}}{r^2}\left\{\frac{r}{a} - \mathrm{arctg}\left(\frac{r}{a}\right)\right\}\frac{\vec{r}}{r}$$

and is determined by the spatial scale a and by the mass M_h inside a sphere of $r < R$. We use the King bulge $\varrho_b = \varrho_{b0}/[1 + (r/b)^2]^{3/2}$, for which the value $M_b = 4\pi b^3 \varrho_{b0}\left\{\ln[(r_b)_{\max}/b + \sqrt{1 + ((r_b)_{\max}/b)^2}] - \frac{(r_b)_{\max}/b}{\sqrt{1 + ((r_b)_{\max}/b)^2}}\right\}$ is the mass of the bulge which inside $r \le (r_b)_{\max}$ yields the force

$$\vec{F}_b = -\frac{4\pi b^3 \varrho_{b0}}{M_b}\left\{\ln\left(\frac{r}{b} + \sqrt{1 + \frac{r^2}{b^2}}\right) - \frac{r/b}{\sqrt{1 + r^2/b^2}}\right\}\frac{M_b}{r^2}\frac{\vec{r}}{r}.$$

It is likely that in the region $r > (r_b)_{\max}$ we have $\vec{F}_b = -M_b\vec{r}/r^3$. These formulae describe a bulge with sharp density decrease. Soft-truncated bulges have been used in the models. The expressions for them are very bulky, and they are not presented.

The surface density of the stellar disk is characterized by the scale L, which defines an exponential law $\sigma(r) = \sigma_0 \exp(-r/L)$. At the distance $r = 5L$ the disk was truncated in accordance with the observational data. We will consider that $R = 4L$.

The vertical structure of the disk is determined by the equation (Bahcall, 1984):

$$\frac{\partial^2\Phi}{\partial z^2} = 4\pi G(\varrho + \varrho_s), \qquad c_z^2\frac{\partial\varrho}{\partial z} = -\frac{\partial\Phi}{\partial z}\varrho.$$

The value ϱ_s is the volume density of matter in spheroidal components. As a result, we obtain an equation for the volume density of the disk $\varrho(z)$

$$\varrho\frac{d}{dz}\left(c_z^2\frac{d\varrho}{dz}\right) - c_z^2\left(\frac{d\varrho}{dz}\right)^2 + 4\pi G(\varrho^3 - \varrho_s(z)\varrho^2) = 0$$

in common with conditions $\varrho(z = 0) = \varrho_0$, $d\varrho(0)/dz = 0$, $\int_{-\infty}^{\infty}\varrho\,dz = \sigma(r, \varphi)$. We have to find ϱ_0 and $\varrho(z)$ at the given $\varrho_s(z)$, $c_z(z)$ and σ. For this purpose construct the function $F(\varrho_0) = 2\int_0^\infty \varrho(z)\,dz - \sigma$. We solve the equation $F(\varrho_0) = 0$ by the iteration method jointly with the numerical integration of the equation for $\varrho(z)$. Then distribute the particles along the z coordinate on the specified grid $z_k = k\Delta z$ ($k = 1, K$). In the kth cell we place the particles

in proportion σ_k/σ, where $\sigma_k = 2\int\limits_{z_{k-1}}^{z_k} \varrho(z)\,dz$ and $\sum\limits_{k=1}^{K} \sigma_k = \sigma$.

The initial equations are written in an approximation $(æ/\omega_z) \ll 1$. The disk thus constructed is not precisely stationary. However, we are investigating the initial unstable states, which evolve to a new stationary state of the disk (if it exists). Therefore, the lack of precise initial balance in the vertical direction plays the part of a slight additional initial disturbance.

The initial function of distribution in velocities is Schwarzschild's, which is anisotropical Maxwell distribution

$$f(u,v,w) = A\,\exp\left\{-\frac{u^2}{2\,c_r^2} - \frac{(v-r\Omega)^2}{2\,c_\varphi^2} - \frac{w^2}{2\,c_z^2}\right\},$$

where $\{u,v,w\}$ are velocity components in the cylindrical coordinate system. The radial component of Jean's equation yields the mean tangential velocity under the assumption $\overline{u} = 0$ and symmetry about $z = 0$:

$$V^2 = (\overline{v})^2 = V_c^2 + c_r^2\left\{1 - \frac{c_\varphi^2}{c_r^2} + \frac{r}{\varrho c_r^2}\frac{\partial(\varrho c_r^2)}{\partial r} + \frac{r}{c_r^2}\frac{\partial(\overline{uw})}{\partial z}\right\},$$

where the circular velocity is defined by the net gravitational potential $V_c^2 = r\left(\dfrac{\partial\Phi}{\partial r}\right)\Big|_{z=0}$ alone, the stroke denotes averaging over the azimuthal coordinate φ.

It should be emphasized that the parameters of the model bar may depend also on the original state of the system, in particular, on the spatial distribution of velocity dispersions in the disk. The way of creation of the bar is not fundamental for us in the given case, it is important that the bar with such parameters can exist in the system.

Fourier-analysis of the surface density in the coordinates φ and $\ln(r)$ furnishes illustrative information for studying bar-like structures. For the Fourier coefficients

$$A(m,p,t) = \frac{1}{N}\sum_{j=1}^{N}\exp\left\{i\left[m\varphi_j(t) + p\ln(r_j(t))\right]\right\},$$

where r_j and φ_j are the radial and azimuthal coordinates of the jth particle, m is the integer, p characterizes twisting of waves. We calculated the versions of $m = 0,1,2,3,4,5,6$ and $p = -20,-19,...,0,1,...,20$. Introduce also integral amplitudes of the Fourier harmonics $\hat{A}(m) = \sqrt{\sum\limits_{p=-15}^{15}|A(m,p)|^2}$, which are convenient when studying the global evolution of the system.

3. Conditions of stabilization of the global bar-mode of late-type galaxies

Two conditions of stabilization of the global bar-mode are most frequently discussed in literature. The central bar is suppressed if the ratio of kinetic energy of chaotic motions of stars (after subtraction of rotation) to potential energy exceeds some critical value $t_{OP} = (E_k/|U|)_{crit} \simeq 0.14$ (Ostriker & Peebles, 1973). It can only slightly depend on the model parameters. It is more important that it is not very convenient to use such a criterion since it includes the unobserved parameters. Numerous data have appeared on determining spatial velocity fields and velocity dispersions in galaxies by the 2D spectroscopy technique, that is why, it is desirable to have a bar stabilization criterion in the form $c_0/V_{max} > (c_0/V_{max})_{crit}$, where c_0 is the radial velocity dispersion of stars at some fixed radius (we will consider that c_0 refers to the centre), V_{max} is the maximum speed of rotation. A simple estimate $0.14 = E_k/|U| \simeq \dfrac{1}{2}\dfrac{c_r^2 + c_\varphi^2 + c_z^2}{GM_D/R} \simeq \dfrac{1}{2}\dfrac{c_r^2}{V_{max}^2}(1 + \alpha_\varphi^2 + \alpha_z^2)$ at $\alpha_\varphi^2 = c_\varphi^2/c_r^2 = 1/2$, $\alpha_z^2 = c_z^2/c_r^2 = 1/4$ yields $c_r/V_{max} \simeq 0.4$, which needs to be refined.

Along with the classical criterion of Ostriker and Peebles (1973), $t_{OP} \simeq 0.14$, other conditions of stability of the global bar-mode (GBM) were put forward. Christodoulou et al. (1995) discussed the condition $\alpha = L\Omega_J/2|U| < 0.25$, here L is the total angular momentum, Ω_J is the Jeans frequency. Some inconvenience of such a kind of criteria is that they are written relative to unobserved parameters. The conditions for the development of the GBM in hot systems deteriorate. Because of this, if the velocity dispersion of stars exceeds some critical value, c_{crit}, the originally axially-symmetric disk proves to be stable. It is more convenient to write such a condition for the radial velocity dispersion c_r, since the dispersion of azimuthal velocities is equal with a good accuracy to $c_\varphi = c_r 2\Omega/æ$ ($\Omega = V_*/r$ is the angular velocity of star rotation, $æ$ is the epicyclic frequency). Besides, the criteria of gravitation stability are written also for c_r.

The global bar-mode is suppressed in the case of massive spheroidal subsystem (halo/bulge). It is customary to assume that the critical ratio is $M_s/M_d|_{crit} \simeq 1$. This result is rather rough and needs specification. The critical value of $M_s/M_d|_{crit}$ is strongly dependent on the ratio of the bulge and halo mass to the disk mass and spatial scales of spheroidal subsystems. We restrict ourselves to the study of models of late-type galaxies, which generally possess a low-mass bulge.

Let us analyse the results of dynamical modeling without a bulge. Since in the halo one should consider

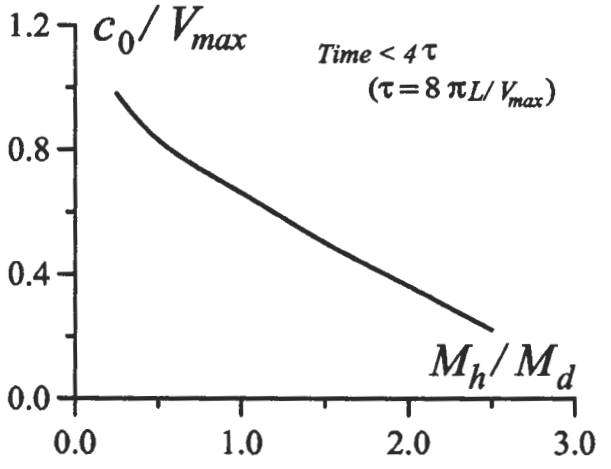

Figure 1: *The dependence of the radial disk velocity dispersion at the centre* $c_o = c_r(r = 0, t = 0)$ *vrs maximum disk rotation velocity upon the halo mass.*

$a \geq L$, the rotation curve in such a potential has then a relatively extended region of increasing. Because of this, gravitational influence of the flat subsystem dominates in the central part of the disk, ($r \lesssim L$), which determines favourable conditions for the development of the bar-mode. Even the massive halo, $1 \leq M_h \leq 2$, is incapable to suppress the global bar-mode if the disk is relatively cold. And only beginning with $M_h \gtrsim 2$ at $a \simeq L$ (M_h is the mass of the halo within the limits of the four exponential scales of the disk) at any small initial dispersions of velocities, the gravitation instability does not lead to formation of a long-lived bar-structure. In the series of experiments, only the halo mass M_h was varied with a spatial scale $a = L$. Fig. 1 shows the dependence of the radial disk velocity dispersion at the centre $c_o = c_r(r = 0, t = 0)$ vrs maximum disk rotation velocity upon the halo mass. It turned out that the global bar-mode instability can form a bar at $M_h/M_d \simeq 2$. In the case the halo is more friable ($a \gtrsim 2L$), the bar is formed when the spheroidal subsystem is even more massive.

Apart from the mechanism of gravitation instability of the global bar-mode, an important part in formation of bars can be played by the instability of radial orbits (Polyachenko, 1992; Polyachenko and Polyachenko, 1996). This mechanism is the most efficient in hot disks with a massive concentrated spheroidal subsystem.

4. Structure of the stellar disk with a bar

4.1. Surface density

Let us examine a self-gravitating disk with a minimum influence of the spheroidal component. If $M_s = 0$, then in the process of heating an important role is played by the mode $m = 1$, which results in displacement of the bar centre with respect to the kinematic centre. In order to avoid this, let us take account of the low-mass bulge with a large scale. Then the effect the bulge has on the development of the global bar-mode will be a minimum.

At the initial time (except for the centre itself) the Toomre parameter is $Q_T \simeq 1$. The disk is unstable with respect to both the global bar-mode and the small-scale Jeans instability. In the initial stage the third mode $m = 3$ dominates. Fig. 2 shows the isolines of surface density and the amplitudes of integral Fourier harmonics $\hat{A}(t)$ for $m = 1, 2, 3, 4, 5, 6$. The arrow indicates domination of the harmonic $m = 3$ in the initial stage of instability development. Such a behaviour is typical enough. It can be assumed that observations of triangular structures may be indicative of the initial stage of development of the gravitation instability leading to formation of a bar structure.

If the distribution of the surface density in the initial time has an exponential profile and the disk is relatively cool (in the final stage the dispersion is about 1.5 as high as the initial), then a marked redistribution of matter in the disk occurs as a result of formation of the bar. Note some characteristic features of this process.

- The disk spreads radially. Up to 30 % of mass may leave the region ($r \lesssim 4L$) occupied originally by matter. The larger M_h, the less mass escapes from this region.
- The resultant profile differs noticeably from the exponential one. The density increases at the centre ($r \lesssim 2L/3$) as compared to the initial profile, and then it decreases (Fig. 3). To derive an exponential density profile, the radial distribution of a special kind should be given (see Fig. 3, dots).

The structure of the bar, its dimension, the ratio of semiaxes and also kinematic characteristics in the central region of the disk depend not only on the rotation curve shape but also on the laws of distribution of matter in disk and spheroidal subsystems. In Fig. 4 are displayed the distributions of isolines of the surface density of the disk subsystem $\sigma(x, y)$ with strongly differing bars and the corresponding curves of rotation and the velocity dispersions of the stellar disk component. This example illustrates that it is rather difficult to understand the structure of a particular galaxy within the frames of common models; one has to construct models for each real object.

4.2. Velocity dispersion

Formation of a bar as a result of development of gravitational instability is accompanied by heating of the disk, which results in increasing velocity dispersion. A

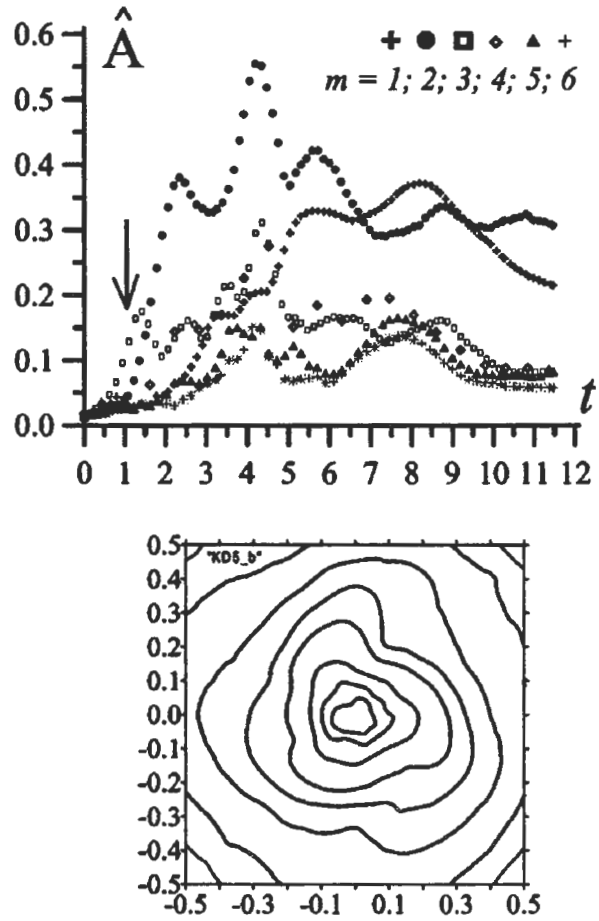

Figure 2: *The upper panel of the figure shows the typical time relation of the integral amplitude of Fourier harmonics for different modes during the bar formation. In the initial stage the third mode, $m = 3$, dominates. The lower panel displays the distribution of the surface density at the time moment $t = 1$.*

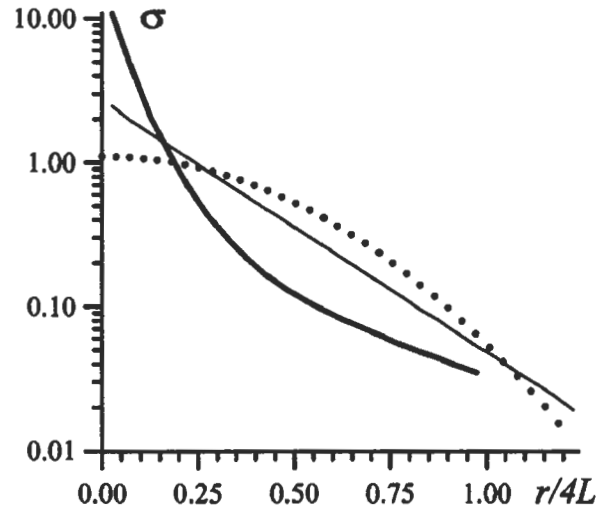

Figure 3: *Radial surface density variation in the disk averaged over the azimuth angle (the thin line is the initial exponential distribution, the bold line is the final profile after formation of the bar, the dots are the initial profile which leads to an exponential relationship at the end of the experiment).*

quasistationary regime is established only after $\simeq 2$ revolutions over the outer edge of the disk. During this time the bar manages to make about 2.5 revolutions.

In an epicyclic approximation (a stationary axially symmetric disk in which the dispersion is small as compared to the rotation velocity) there must be a simple relation between the dispersion components (Vandervoort, 1970):

$$c_\varphi(r) = \frac{æ(r)}{2\,\Omega(r)}\, c_r(r)\,.$$

One would think that in a disk with a bar the epicyclic approximation is obviously disturbed. However, it turned out in dynamical modeling that in a hot non-axisymmetric disk with a bar $Q_c = c_r æ/(2\Omega c_\varphi) \simeq 1$ not only at the end of calculation under the condition of quasistationary state but also during the whole stage of formation of the bar structure (Fig. 5).

Fig 6 shows the isolines of three velocity dispersion components of matter in the disk, c_r, c_φ, c_z. The surface density distribution depicted in Fig. 4 on the left corresponds to them. Each velocity dispersion component has its characteristic distribution which is typical of the bar-mode irrespective on the conditions of the experiment. Note that unlike the surface density, the radial velocity dispersion distribution conserves two spiral arms. At the same time, the dimension of the "bar" from the distribution of the c_r is approximately twice as small as that in the surface density. The spatial distribution of the azimuthal velocity dispersion c_φ differs markedly from $c_r(x, y)$ for which an elongated structure at the centre is characteristic. The half-thickness of the disk h does not establish the identity of a bar-structure.

The velocity dispersion along the line of sight depends on the mutual orientation of the disk and bar according to the formula

$$c_{obs} = \sqrt{c_z^2 \cos^2(i) + c_\varphi^2 \sin^2(i)\cos^2(\alpha) + c_r^2 \sin^2(i)\sin^2(\alpha)}\,,$$

where α is the azimuthal angle reckoned from the major axis in the galaxy plane, Fig. 7 shows the velocity dispersion distribution along the line of sight at different angles of disk inclination ($i = 30°, 60°$) and orientations of the major axis of the disk and the bar. If the major axes of the bar and galaxy coincide (see Fig. 7*c*, *d*), then the dispersion distribution does not reveal any bar-structure. At other orientations of the bar and major axes of the galaxy, elongated structures in the field of c_{obs} are pronounced. The "bar-structure" of the velocity dispersion in all the

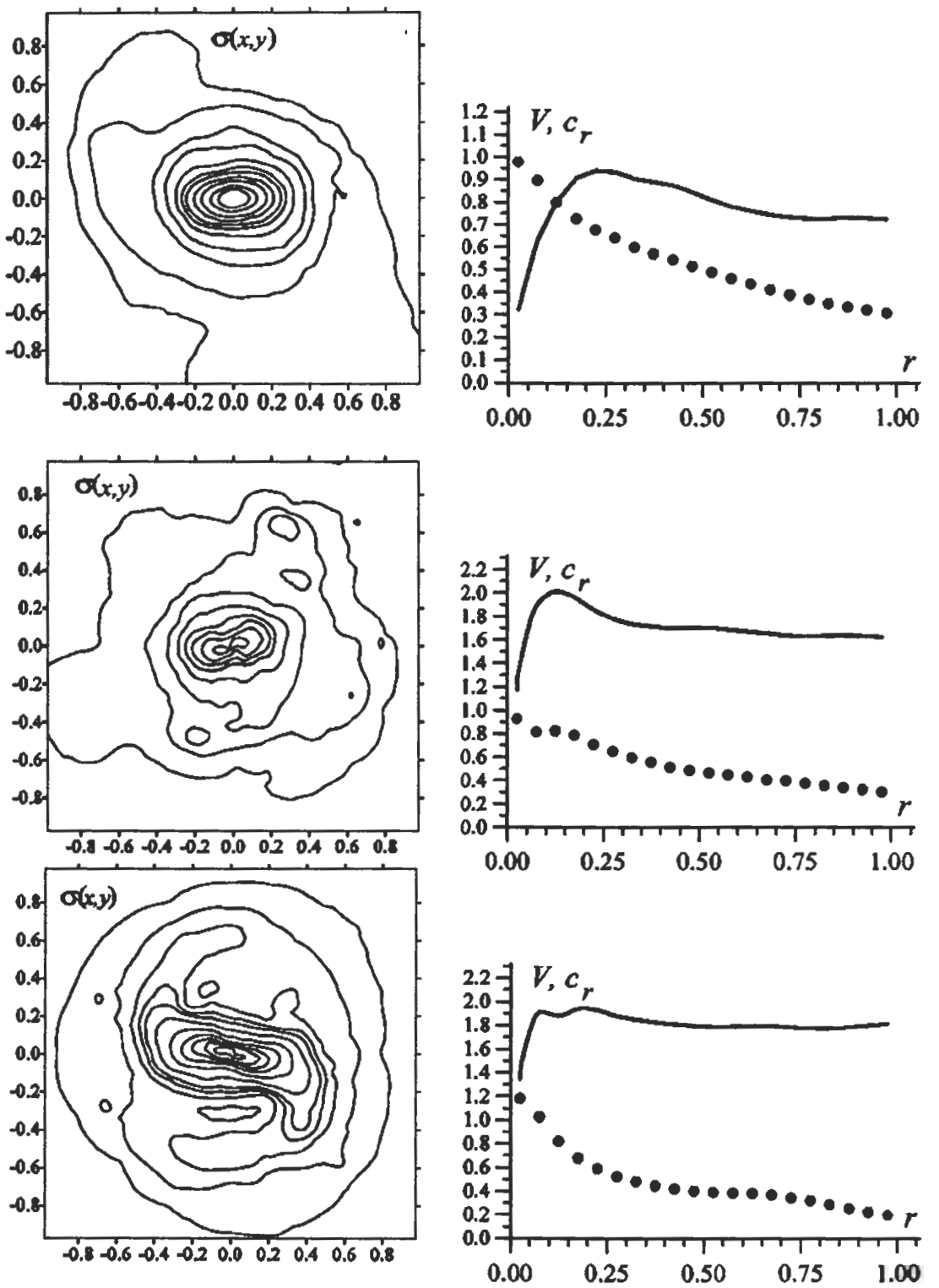

Figure 4: *The left panels are the isolines of the surface density inside the radius* $r = 4L$. *The right panels display the corresponding rotation curves of the disk matter* $V(r)$ *(the line) and the radial velocity dispersions* $c_r(r)$ *(the dots).*

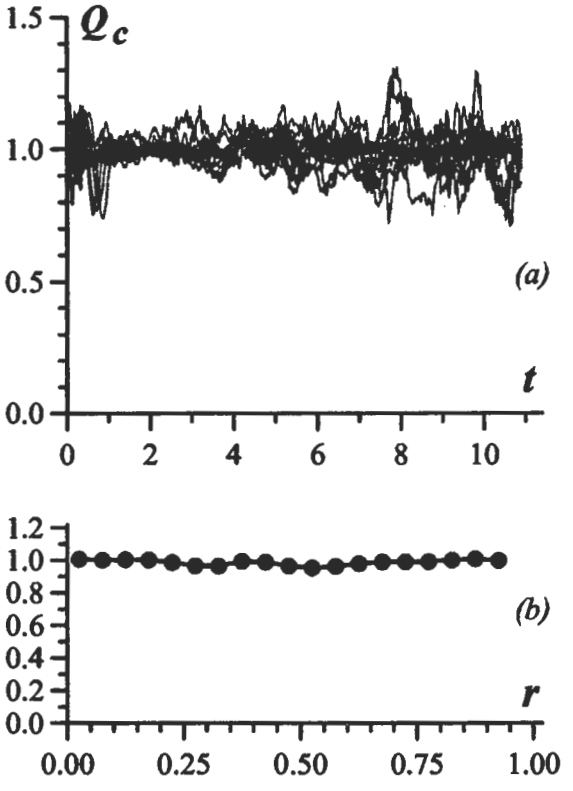

Figure 5: *The parameter Q_c as a function of time (a), the time-averaged radial relationship Q_c (b).*

cases is of small size in comparison with the surface density bar. All other things being equal, the velocity dispersion bar is more pronounced at larger inclination angles i, which is related to diminishing of the contribution of the vertical velocity dispersion c_z to c_{obs}. Note that the distributions of different velocity dispersion components, c_r, c_φ, c_z, in the case of presence of a massive bulge remain bearing resemblance to those depicted in Fig. 7.

5. Examples of modeling stellar disks with bars

We will describe in this section dynamical models of three galaxies. If we coordinate the observed rotation curves and velocity dispersions with the kinematic data obtained in the numerical experiment, it will be possible then to determine the spatial distribution of matter in the bulge and halo (Khoperskov et al., 2001). Such an approach was implemented for a number of galaxies without the bar. We will discuss here SB galaxies.

Unfortunately, all kinematic data of the central region have a relative large uncertainties (especially the velocity dispersion of stars). For this reason, the results obtained should be taken as estimating.

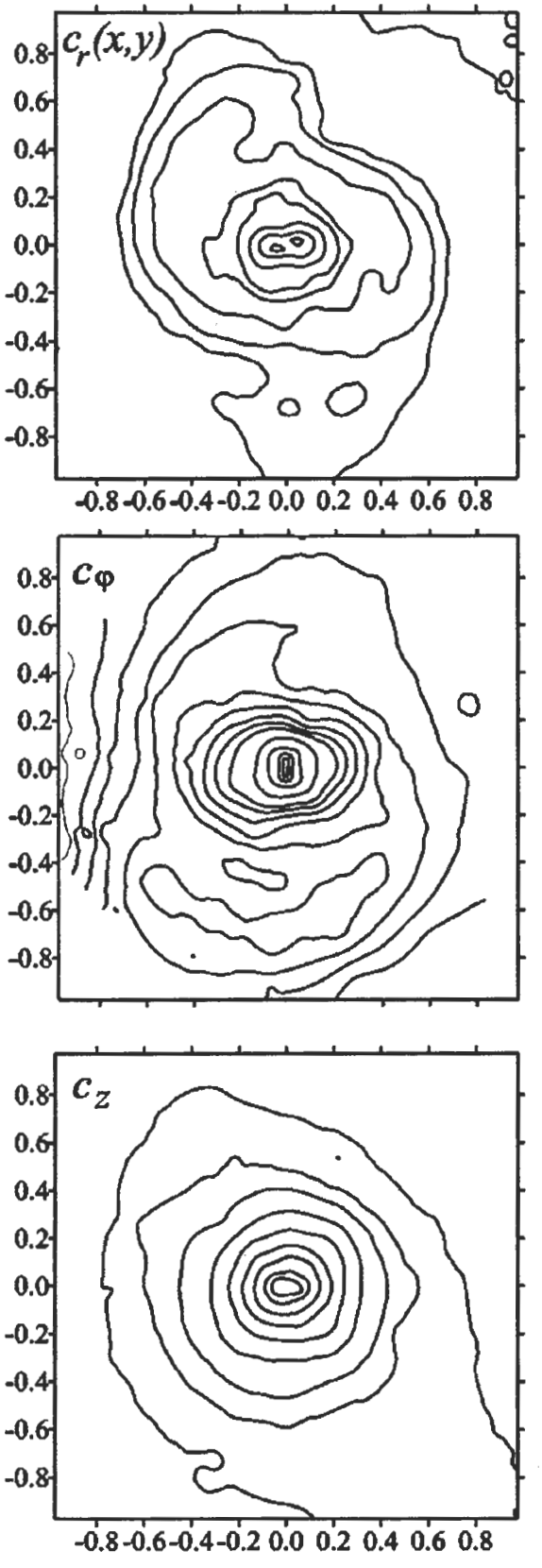

Figure 6: *The distribution of the dispersions of radial, azimuthal and vertical velocity components in the disk plane in the presence of the bar. The surface density distribution corresponding to this case is given in Fig. 4 (left).*

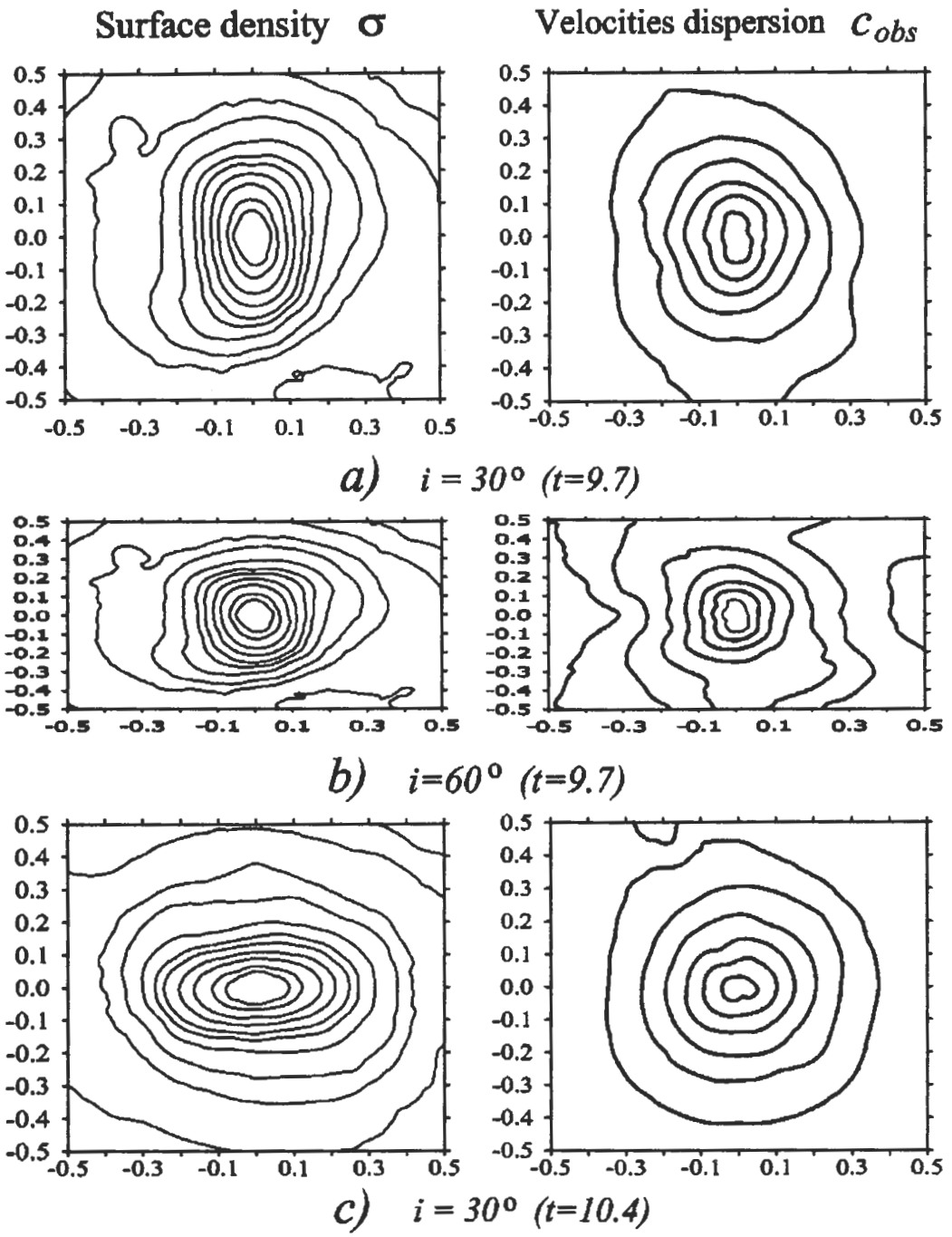

Figure 7: *The velocity dispersion distribution of the disk matter along the line of sight at different inclination angles of the disk: a, b — the major axis and the bar are perpendicular; c, d — the major axis and the bar are parallel; e, f — the angle of the major axis with the bar is* 45°.

5.1. NGC 936

We will use the observed rotation curves V_{gas} and V_* and the velocity dispersion of stars c_{obs} of Kormendy (1984). NGC 936 belongs to lenticular galaxies, which provides for a massive enough central component. Let us choose the disk scale $L = 3.7$ kpc, the bar radius is $r_{bar} = 4.1$ kpc, and the inclination angle $i = 41°$. The given galaxy is a rare object for which attempts are known to find the angular velocity of bar rotation directly from the observed velocity field. From the data of Merrifield and Kuijken (1995) $\Omega_{bar} = 60 \pm 14$ km/s/kpc. However in the paper by Kent (1987) it was found that $\Omega_{bar} = 104 \pm 37$ km/s/kpc.

In Fig. 8 are shown the results of dynamical modeling. In the central region, comparison was made by the rotation velocity of the stellar component,

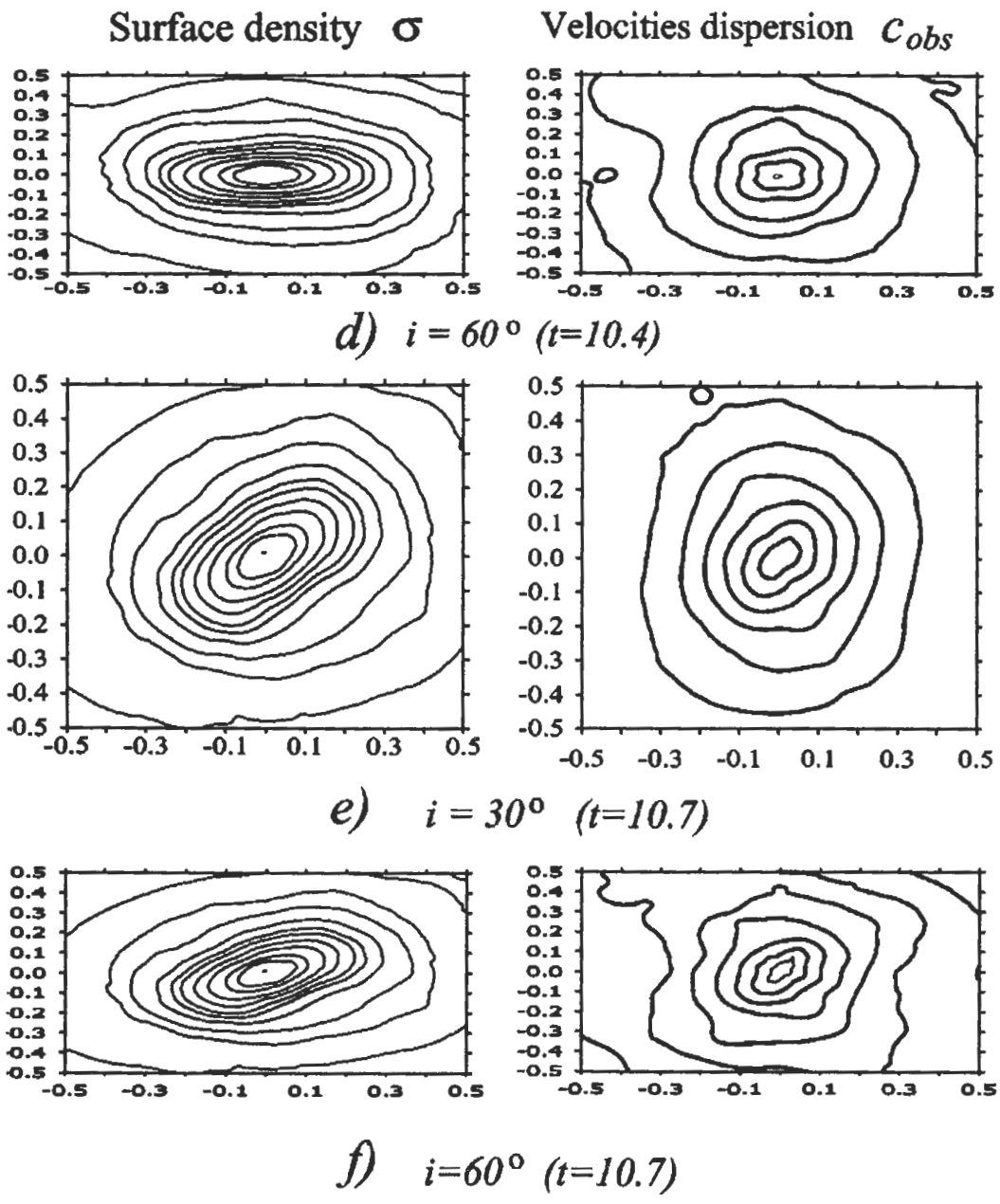

Figure 7: *(continued)*

at the periphery it was made by the velocity of rotation of gas. Satisfactory agreement turns out at the disk mass $M_d = 16.7 \cdot 10^{10} M_\odot$, the halo mass $M_h = 17.8 \cdot 10^{10} M_\odot$ with a scale $a = 5.12$ kpc, the mass of the nucleus $M_c = 0.21 \cdot 10^{10} M_\odot$ with a scale $b_1 = 0.22$ kpc ($(r_{b1})_{\max} = 0.46$ kpc), the bulge mass $M_b = 3 \cdot 10^{10} M_\odot$ with a scale $b_2 = 1.57$ kpc ($(r_{b2})_{\max} = 3.2$ kpc).

Attempts to derive dynamical models of NGC 936 had been undertaken earlier (Sparke & Sellwood, 1987), but apart from the bar a powerful two-armed stellar spiral was formed according to the derived model, which is not observed in the lenticular galaxy NGC 936. Besides, no agreement with the observed kinematic parameters was carried out.

5.2. NGC 1169

The galaxy NGC 1169 is classified as SABb(r) (de Vaucouleurs et al., 1991). When constructing a dynamical model, the exponential scale was assumed to be $L = 4.31$ kpc, the inclination angle $i = 53°$, the bar radius $r_{bar} = 6.06$ kpc, the axes ratio of the bar was assumed to be equal to 0.6. The variation of the gas velocity rotation along the radius is known beyond the radius $r = 10$ kpc (van Driel & van Woerden, 1994). The data on the rotation velocity of stars

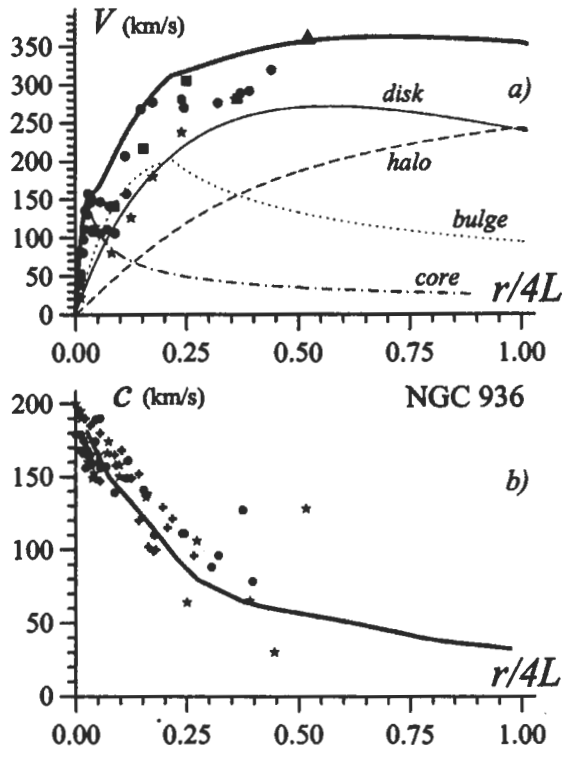

Figure 8: *The results of construction of the dynamical model for the galaxy NGC 936 (the lines). Different symbols indicate the observational data (Kormendy, 1984).*

refer to the central region, $r < 3.6\,\mathrm{kpc}$ (Heraudeau & Simien, 1998). A dynamical model has been constructed which describes best the aggregate of observational data. The total mass within $r \leq 4L = 17.22\,\mathrm{kpc}$ makes $M_{tot} = 2.8 \cdot 10^{11}\,M_\odot$. It is the sum of $M_d = 0.952 \cdot 10^{11}\,M_\odot$, $M_b = 0.093 \cdot 10^{11}\,M_\odot$, $M_h = 1.749 \cdot 10^{11}\,M_\odot$. The halo is massive, $M_h/M_d = 1.8$, but the halo scale, $a = 7.11\,\mathrm{kpc}$, exceeds considerably the disk scale. This facilitates the formation of the bar as a result of development of instability of the global bar-mode. Within the two disk scales the effect the halo has on the rotation curve is small, and only beyond $12.5\,\mathrm{kpc} = 3L$ the contribution of the halo begins to dominate.

We have not been able to obtain the odserved velocity dispersion $c_{obs} = 150 \div 200\,\mathrm{km/s}$ in the region $r < 0.5L \simeq 2.1\,\mathrm{kpc}$ within the dynamical model. This, apparently, implies that the contribution of bulge stars to the observed velocity dispersion is considerable here. And even in the zone $0.5L < r < L$ the bulge influence is small and c_{obs} and c_{exp} are in agreement. The parameters of the bulge obtained in the dynamical model ($M_b/M_d = 0.098$, $b = 0.32\,\mathrm{kpc}$, $(r_b)_{\max} = 3.2\,\mathrm{kpc}$) appear to be very close to the results of decomposition of the brightness profile ($M_b/M_d = 0.12$, $b = 0.319\,\mathrm{kpc}$, $(r_b)_{\max} = 3.224\,\mathrm{kpc}$). Our estimate of the total mass within $r = 29\,\mathrm{kpc}$, $M_{tot} = 4.9 \cdot 10^{11}\,M_\odot$ is not at variance with the conclusions of van Driel & van Woerden (1994) who obtained $M_{tot} = 4.5 \cdot 10^{11}\,M_\odot$.

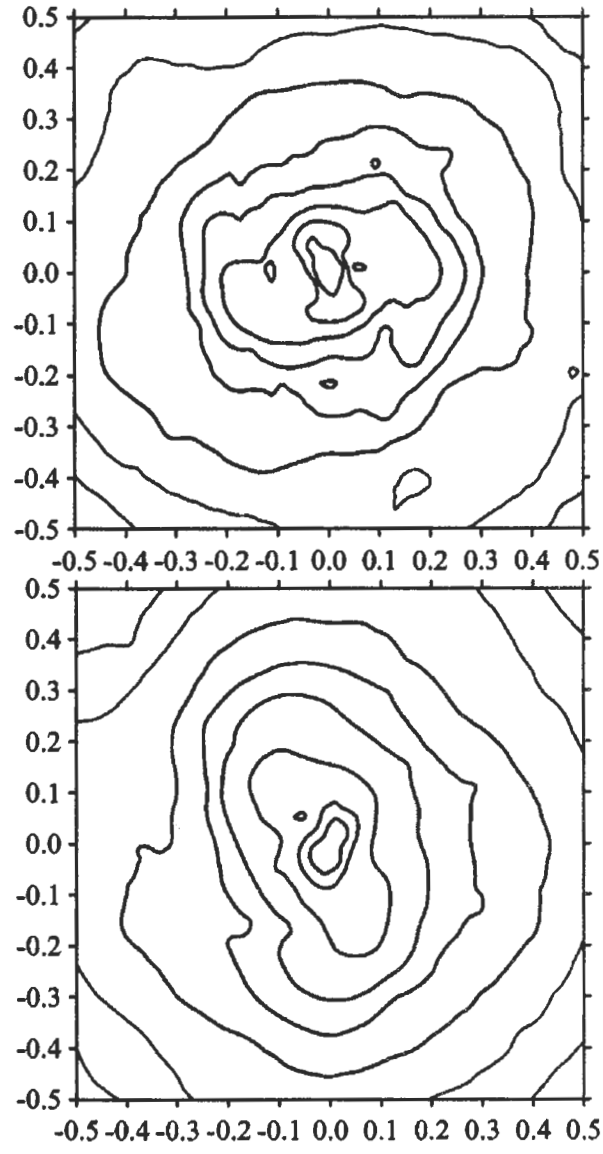

Figure 9: *The central part of the disk ($r < 2L$) of some dynamical models. Isolines of the surface density are shown.*

5.3. NGC 2712

The results of the brightness profile decomposition for NGC 2712 yield $L = 2.44\,\mathrm{kpc}$, $b = 0.194\,\mathrm{kpc}$, $(r_b)_{\max} = 2.961\,\mathrm{kpc}$, $M_b/M_d = 0.055$, $i = 60°$. The parameters of the bar: $r_{bar} = 4.72\,\mathrm{kpc}$, the axial ratio is 0.4.

We will use the rotation curve of the gas component, V_{gas}, obtained by Márquez and Moles (1996). We borrow V_* and c_{obs} from the paper by Heraudeau et al. (1999).

The dynamical model with the bulge parameters obtained from the photometric decomposition agree poorly with the kinematic data at the centre. Here we have been unable to derive the observed parameters of the bar. This is why, we have constructed models with other parameters of the bulge. When the mass of the bulge is increased to $M_b/M_d = 0.13$, this model has then a better fit to the observations in the central region. The best fit has been derived in a more complex model of the central spheroidal subsystem consisting of a nucleus ($M_c = 1.34 \cdot 10^9\, M_\odot$ kpc, $b_1 = 0.18$ kpc, $(r_{b1})_{\max} = 0.56$ kpc) and a bulge ($M_b = 3.14 \cdot 10^9\, M_\odot$, $b_2 = 0.78$ kpc, $(r_{b2})_{\max} = 1.56$ kpc).

6. Double bars

In the process of dynamical modeling under certain conditions structures are formed that can be interpreted as double bars (Fig. 9). Nested "bar" can make an arbitrary angle to the main one. However, the lifetime of such structures is not long. They are formed in final stages of development of gravitation instability, generally at sufficiently massive spheroidal components. If double bars are really dynamical structures then the relatively rare frequency of occurrence of such systems becomes explainable.

Acknowledgements. This work was supported by the RFBR grant (project No. 01-02-17597).

References

Bahcall J.N., 1984, Astrophys. J., **276**, 156
Christodoulou D.M., Shlosman I., Tohline J.E., 1995, Astrophys. J., **443**, 563
van Driel W., van Woerden H., 1994, Astron. Astrophys., **286**, 395
Heraudeau Ph., Simien F., 1998, Astron. Astrophys. Suppl. Ser., **133**, 317
Heraudeau Ph., Simien F., Maubon G., Prugniel Ph., 1999, Astron. Astrophys. Suppl. Ser., **136**, 509
Kalnajs A.J., 1987, in: IAU Symp. 117, "Dark matter in the Universe", Dordrecht, 289
Kent S.M. 1987, Astron. J., **93**, 816.
Khoperskov A.V., Zasov A.V., Tiurina N.V., 2001, Astron. Zh., (in press)
Kormendy J., 1984, Astrophys. J., **286**, 132
Márquez I., Moles M., 1996, Astron. Astrophys. Suppl. Ser., **120**, 1
Merrifield M.R., Kuijken K., 1995, Mon. Not. R. Astron. Soc., **274**, 933
Moiseev A.V., 1998, Prepr. SAO, No.134
Ostriker J.P., Peebles P.J.E., 1973, Astrophys. J., **186**, 467
Polyachenko V.L., 1992, Astron. Zh., **69**, 10
Polyachenko V.L., Polyachenko E.V., 1996, Pis'ma Astron. Zh., **22**, 337
Sparke L.S., Sellwood J.A., 1987, Mon. Not. R. Astron. Soc., **225**, 653
Tremaine S., Weinberg M.D., 1984, Astrophys. J., **282**, L5
Vandervoort P.O., 1970, Astrophys. J., **161**, 67
de Vaucouleurs G., de Vaucouleurs A., Corwin H.C., 1991, Third Reference Catalogue of Bright Galaxies. Reidel, New York.
Weinberg M.D., 1992, Astrophys. J., **384**, 81